Aeolian Research 70-71 (2024) 100941

Contents lists available at ScienceDirect

Aeolian Research

journal homepage: www.elsevier.com/locate/aeolia

Full Length Article

Characterizing variability in geochemistry and mineralogy of western US dust sources

Abby L. Mangum [a], Gregory T. Carling [a,*], Barry R. Bickmore [a], Nicholas Webb [b], DeTiare L. Leifi [c], Janice Brahney [d], Diego P. Fernandez [e], Kevin A. Rey [a], Stephen T. Nelson [a], Landon Burgener [a], Joshua J. LeMonte [a], Alyssa N. Thompson [a], Beth A. Newingham [f], Michael C. Duniway [g], Zachary T. Aanderud [c]

[a] Department of Geological Sciences, Brigham Young University, Provo, UT, USA
[b] USDA-ARS Jornada Experimental Range, Las Cruces, NM, USA
[c] Department of Plant & Wildlife Sciences, Brigham Young University, Provo, UT, USA
[d] Department of Watershed Sciences and Ecology Center, Utah State University, Logan, UT, USA
[e] Department of Geology & Geophysics, University of Utah, Salt Lake City, UT, USA
[f] USDA-ARS Great Basin Rangelands Research, Reno, NV, USA
[g] US Geological Survey, Southwest Biological Science Center, Moab, UT, USA

ARTICLE INFO

Keywords:
National Wind Erosion Research Network
Western US
Dust geochemistry
Dust mineralogy
Dust tracking
Linear discriminant analysis

ABSTRACT

Dust events originate from multiple sources in arid and semi-arid regions, making it difficult to quantify source contributions. Dust geochemical/mineralogical composition, if the sources are sufficiently distinct, can be used to quantify the contributions from different sources. To test the viability of using geochemical and mineralogical measurements to separate dust-emitting sites, we used dust samples collected between 2018 and 2020 from ten National Wind Erosion Research Network (NWERN) sites that are representative of western United States (US) dust sources. Dust composition varied seasonally at many of the sites, but within-site variability was smaller than across-site variability, indicating that the geochemical signatures are robust over time. It was not possible to separate all the sites using commonly applied principal component analysis (PCA) and cluster analysis because of overlap in dust geochemistry. However, a linear discriminant analysis (LDA) successfully separated all sites based on their geochemistry, suggesting that LDA may prove useful for separating dust sources that cannot be separated using PCA or other methods. Further, an LDA based on mineralogical data separated most sites using only a limited number of mineral phases that were readily explained by the local geologic setting. Taken together, the geochemical and mineralogical measurements generated distinct signatures of dust emissions across NWERN sites. If expanded to include a broader range of sites across the western US, a library of geochemical and mineralogical data may serve as a basis to track and quantify dust contributions from these sources.

Introduction

Dust emissions originate from multiple sources in arid and semi-arid regions and are mixed in the atmosphere before being deposited. Identifying dust origin is often difficult because information about dust source composition is lacking, or single isotopic/elemental indicators have overlapping signatures in source areas, leaving ambiguity in identifying source areas (Grousset and Biscaye, 2005). Dust geochemistry is controlled by the composition of underlying soils and bedrock and is influenced by anthropogenic inputs (Goodman et al., 2019; Reheis et al., 2009). Thus, dust source tracking traditionally utilizes radiogenic and stable isotopes (Blakowski et al., 2016; Carling et al., 2020; Munroe et al., 2019; Nakano et al., 2004), geochemistry (Guinoiseau et al., 2022), mineralogy (Chen and Li, 2011; Menéndez et al., 2014), and microbes (Abed et al., 2012; Dastrup et al., 2018). A compilation of the physicochemical properties of dust emitted from relevant source regions is needed to unmix dust samples and trace dust events or deposited dust back to its source. Combining isotopic, geochemical, mineralogical, and microbial measurements on samples from representative dust source regions may provide sufficient information for apportionment of mixed

* Corresponding author.
E-mail address: greg.carling@byu.edu (G.T. Carling).

https://doi.org/10.1016/j.aeolia.2024.100941
Received 23 May 2024; Received in revised form 13 September 2024; Accepted 16 September 2024
Available online 21 September 2024

samples in depositional areas. A better understanding of dust source areas may inform land-use policy for mitigating dust, lead to better decisions regarding dust hazard mitigation, and assist with air quality improvements in downwind populated areas.

Dust emissions are controlled by a variety of factors, which may change seasonally or interannually, with impacts on downwind ecosystems. Factors affecting dust emissions include vegetation cover, biocrusts, precipitation, wind velocity, landscape disturbance, and soil moisture (Belnap et al., 2009; Belnap et al., 2014; Pierre et al., 2012). Dust production is diverse across Earth's surface with source regions occurring in a variety of environments and land use types (Prospero et al., 2002). Important dust sources include playas, bare land, overgrazed areas, areas with heavy industry, and unpaved roads (Brahney et al., 2015; Carling et al., 2020; Duniway et al., 2019; Middleton and Goudie, 2001). Increased livestock grazing in the western United States (US) over the past two centuries was linked to higher rates of dust deposition to downwind areas (Neff et al., 2008). The increased dust loading leads to eutrophication of alpine lakes and other water bodies (Brahney et al., 2015; Zhang, 1994), earlier snowmelt and decreased runoff from mountain snowpack (Painter et al., 2010; Skiles et al., 2015), and negative effects on air and water quality (Dastrup et al., 2018; Goodman et al., 2019; Kellogg and Griffin, 2006; Marcy et al., 2024; McTainsh and Strong, 2007; Putman et al., 2022).

Dust from different source areas may be distinguished based on its geochemical and mineralogical composition. A common method for evaluating variability in dust composition is with trace element concentrations (Ben-Israel et al., 2015; Brahney et al., 2019; Marx et al., 2008; Zhao et al., 2015). Multivariate statistical tools, such as principal component analysis (PCA), are often used to interpret large geochemical datasets and compare mixed dust to various sources (Chen et al., 2022; Goodman et al., 2019; Heindel et al., 2020; Marcy et al., 2024; Putman et al., 2022; Zeng et al., 2022). Variations in dust mineralogy on a regional scale are often subtle, and in some cases may not be distinct enough to identify source areas (Lawrence and Neff, 2009). Assemblages of low-density minerals, such as quartz, K-feldspar, and plagioclase, are useful tracers because they are major components of aeolian dust and likely undergo minimal fractionation during wind transport (Chen and Li, 2011).

To develop endmember libraries for dust tracing studies in the western US, we differentiated representative dust sources based on distinct geochemical and mineralogical compositions. For effective unmixing, endmembers must be compositionally distinct and remain stable through time. Our specific objectives were to develop geochemical and mineralogical signatures of representative dust source areas and to investigate the seasonality of the signatures. To accomplish these objectives, we measured trace and major element concentrations and mineral abundances in seasonal samples collected by the National Wind Erosion Research Network (NWERN) (https://www.winderosionnetwork.org), which is a collaborative effort to create a long-term research program to address critical challenges in wind erosion research and land management in the US (Webb et al., 2016). The network aims to provide data to understand basic aeolian processes across various land use types and management practices, develop models to assess wind erosion and dust emissions, and encourage collaboration in the aeolian research community (Webb et al., 2016). The NWERN sites collect data on saltation and dust emission fluxes, but until now have not evaluated dust geochemical and mineralogical composition.

2. Materials and methods

2.1. Dust sample collection

To evaluate the composition of dust emissions across the western US, we obtained 122 composited samples from ten representative NWERN sites, including samples from Nevada (Red Hills and Twin Valley), Utah (Moab), Colorado (Central Plains Experimental Range—CPER and Akron), New Mexico (Lordsburg, Jornada, and Holloman Air Force Base—HAFB), North Dakota (Mandan), and Oklahoma (El Reno) (Fig. 1). The sites include playa, rangeland, and cropland land use types. Site and sampling details are provided in Table 1 and in the Supplementary material (Table S1).

Dust composite samples were collected using Modified Wilson and Cooke (MWAC) samplers. Each NWERN site has 27 MWAC sampler masts with three masts randomly placed in each of nine regular grids used to stratify the one-hectare sites (Webb et al., 2019). Wind vanes on the MWAC masts direct airborne sediment into the collectors. The MWAC masts hold naturally-aspirated MWAC samplers situated at four different heights above ground level (10 cm, 25 cm, 50 cm, 80 cm) to measure the horizontal sediment flux (Webb and Herrick, 2015). The MWAC samplers were emptied monthly according to NWERN protocols (Webb and Herrick, 2015) and stored in clean plastic vials and bags for laboratory analyses. At the time of storage, samples from individual MWAC masts and sampler heights were composited by height into three sample groups. Composite samples were formed by combining all samples at each of the respective heights (10 cm, 25 cm, 50 cm, 85 cm) collected at the first, second, and third MWAC masts across the grid cells (Webb and Herrick, 2015). The MWAC samplers are generally efficient at trapping dust, but the efficiency depends on wind speed and particle size so that the samplers may be biased towards collecting larger particles (Goossens and Offer, 2000). To more effectively analyze smaller dust particles that are more likely suspended over longer distances, we focused on composited samples from the two highest MWAC samplers (e.g., 50 cm and 85 cm above ground surface) at each NWERN site. Compositing dust samples ensured that we captured spatial variability of the sediment mass fluxes and chemistry of dust sampled within each NWERN site. Bulk samples were used for all geochemical and mineralogical analyses because there was insufficient material for all samples to be separated into smaller size fractions.

The composited dust samples were collected between 2018 and 2020 and were consolidated by season (spring, summer, and fall). Spring samples were collected from March to May, summer samples were collected from June to August, and fall samples were collected from September to November. The number of composited samples collected during each season from each site is provided in the Supplementary material (Table S1).

2.2. Laboratory analyses

To measure trace and major element concentrations, dust samples were digested using aqua regia and analyzed by inductively coupled plasma-mass spectrometry (ICP-MS). Specifically, ~50 mg of dust from each sample was split into acid-washed 15 mL centrifuge tubes. An aqua regia mixture (1.33 mL HCl and 0.67 mL HNO_3, using concentrated trace metal grade acids) was added to each sample. The samples were stirred vigorously and left to equilibrate for ~24 h at room temperature. After digestion, the samples were diluted with 10 mL of 18.2 MΩ-cm ultrapure water and centrifuged at 3000 rpm for five minutes. The sample digestion targeted minerals such as carbonates, feldspars, clays, and silicates, although not all silicate and refractory minerals were completely dissolved (Goodman et al., 2019).

The supernatant from the diluted aqua regia digestate was analyzed for trace and major element concentrations using a triple quadrupole ICP-MS (Agilent 8900, Agilent Technologies, Santa Clara, CA, USA). Concentrations were quantified using an external calibration curve for the following 44 elements: Li, Be, B, Na, Mg, Al, K, Ca, Sc, V, Cr, Mn, Fe, Co, Ni, Cu, Zn, Se, Rb, Sr, Y, As, Mo, Cd, Sb, Cs, Ba, La, Ce, Pr, Nd, Sm, Eu, Gd, Tb, Dy, Ho, Er, Yb, Lu, Tl, Pb, Th, and U. The external calibration curve was prepared from commercially available 1,000 mg L^{-1} single-element standards, with maximum concentrations around 0.1 mg L^{-1} for trace elements and 10 mg L^{-1} for major elements (Inorganic Ventures, Christiansburg, VA, USA). The ICP-MS instrument uses a dual pass

Fig. 1. Map of the ten included National Wind Erosion Research Network (NWERN) sites across the western United States.

Table 1
Site characteristics and number of composited dust samples collected at ten National Wind Erosion Research Network (NWERN) sites.

Site	State	Annual precip[1] (mm)	Elevation[1] (m asl)	Land use type[1]	Local substrate[2]	Composited samples (*n*)
Akron	Colorado	421	1383	Cropland	Claystone, sandstone	6
CPER	Colorado	320	1650	Rangeland	Shale, sandstone	11
El Reno	Oklahoma	815	420	Cropland	Shale, sandstone	5
HAFB	New Mexico	278	1267	Playa/rangeland	Alluvium, gypsum sand	24
Jornada	New Mexico	250	1320	Rangeland	Alluvium, sand, gravel	19
Lordsburg	New Mexico	286	1267	Playa	Lacustrine deposits	3
Mandan	North Dakota	410	591	Cropland	Glacial till, mudstone	3
Moab	Utah	229	1575	Rangeland	Sand, sandstone	24
Red Hills	Nevada	200	1725	Rangeland	Basalt, rhyolite	12
Twin Valley	Nevada	200	1668	Rangeland	Basalt	15

[1] https://winderosionnetwork.org/.
[2] Geologic maps provided in the Supplementary material.

quartz spray chamber, PTFE nebulizer and dual-syringe introduction system, platinum cones, and sapphire injector in a platinum-shielded quartz torch. Detection limits for each element were calculated as three times the standard deviation of the background, multiplied by the total dilution factor used for samples (~2,000). A standard reference material (SRM 1643f, Trace Elements in Water, National Institute of Standards and Technology) was analyzed multiple times in each run together with the samples as a continuing calibration verification. The long-term reproducibility for SRM 1643f shows that our results are accurate within 5 % for most elements, with measured values well above the method detection limits.

Mineralogy was analyzed by X-ray powder diffraction (XRD) for 85 dust samples that had sufficient material remaining after splitting for geochemical analyses. Samples were ground, wet-milled in a McCrone XRD Mill, dried, shaken in a non-polar solvent (Vertrel), passed through a 60-mesh sieve, mounted on zero-background holders, and analyzed with a Rigaku MiniFlex 600 X-ray diffractometer (Eberl, 2003). Resulting patterns were quantitatively interpreted from the reference intensity ratio (RIR) method with the Rigaku PDXL2 software. For the RIR method, weight ratios were calculated from given intensity ratios of the substance normalized to a known standard and its highest peak intensity (Hubbard et al., 1976). The RIR method provides a basic mineralogical analysis, but due to limited sample size we were unable to obtain detailed information on clay minerals. In the mineralogical data set, minerals difficult to differentiate from one another in random-mount X-ray diffractograms of mineral mixtures were grouped to make the analyses more robust against mineral misidentification. The mineral groups were K-feldspars (microcline, orthoclase, and sanidine), Na-feldspars (sodic plagioclase and anorthoclase), smectites (montmorillonite and nontronite), and 2:1 phyllosilicates (smectite, illite, muscovite, and biotite). However, other detected minerals were not grouped.

All raw data generated for trace and major element concentrations and mineralogy are provided in Mangum et al. (2024).

2.3. Multivariate statistics

To identify distinct geochemical or mineralogical signatures across the NWERN sites, we applied three multivariate statistical approaches (cluster analysis, PCA, and linear discriminant analysis) using analytical tools from the pandas (Zenodo, 2024) and scikit-learn (Pedregosa et al., 2011) Python packages. In all cases, we used normalized (z-scored) data to avoid the algorithms being unduly influenced by variables with larger numbers.

A hierarchical cluster dendrogram of the geochemical data arranged the samples in order of Euclidean distance from one another in normalized data space. This allowed us to determine whether the samples from individual sites were all closer to each other than to those from any other sites. The weakness of this approach in this context is that data within the categories of interest (sample locations) might be completely separable from the other categories, but some of the individual data points might still be closer to data points from other categories than to data points within the group (Davis, 2002).

A PCA was applied to the geochemical data to determine whether data from different sites could be separated based on the most important directions in the normalized data, in terms of variance explained. PCA is an unsupervised technique in which the multi-dimensional axes of normalized data space are rotated to incorporate the most possible data variance in the fewest possible axis directions (Davis, 2002). The weakness of this approach in this context is that the directions in data space that explain the most variance are not necessarily the best directions for separating the categories of interest (sample locations) (Davis, 2002).

We performed linear discriminant analysis (LDA) on both the geochemical and mineralogical data, using the sample sites as target categories. An additional LDA was performed using only the rare earth element (REE) and Y concentrations to test the sensitivity of the LDA to the number of variables used as inputs. LDA is similar to PCA, in that it provides a set of rotated axes (linear discriminants) in normalized data space, ordered by variance explained. But since LDA is a supervised technique, the directions of the linear discriminants are specifically chosen for their usefulness in separating the target categories (Davis, 2002). In addition, for each site with greater than ten composite samples, we performed an LDA to see if the individual sites' elemental data could be differentiated based on season. Coefficients for the principal components (PCs) and linear discriminants (LDs) are provided in the Supplementary material (Tables S2–S6).

Prior to running the statistical analyses, steps were taken to clean the data. For example, non-detect values were set to ½ the detection limit for each element. Although it is arbitrary, adjusting the non-detect values was justified because it only impacted a few samples/elements (7 samples for B, 2 for Sc, and 1 for Se). One sample (DTL-14 from CPER) was excluded from the statistical analyses because it had anomalously high concentrations of Cu and Zn, likely due to contamination during sample collection or processing.

2.4. Geologic maps of study sites

Geologic maps for each study site were compiled using ArcGIS Pro (Esri, 2024). Reference maps were obtained from state geologic survey websites or the US Geological Survey (USGS) (Doelling, 2002; Miser, 1954; Murphy, 1999; Ogden, 1979; Scholle, 2003; Stewart and Carlson, 1978). In cases where geographic information system (GIS) databases and shapefiles were unavailable, static images of geologic maps were georeferenced and traced to create unique polygon feature classes of the relevant geologic units. Colors were standardized across geologic maps according to the official USGS colors (USGS, 2005). Geologic maps are provided in the Supplementary material.

3. Results

3.1. Trace and major element chemistry show variability across NWERN sites

Elemental concentrations in dust varied across the ten NWERN sites. For example, the Lordsburg playa site had the highest concentrations of Li, Cu, Se, Mo, REE + Y, Th, and U. The HAFB site had the highest concentrations of B, Mg, Ca, Ni, Sr, and Mo. Both Lordsburg and HAFB spring samples had elevated Na concentrations. Dust from the Red Hills and Twin Valley sites in Nevada had the highest Mn concentrations. The Red Hills site also had the highest Ba concentrations. Dust from four sites, Lordsburg, Red Hills, Twin Valley, and Mandan, had relatively high As and Cs concentrations. These four sites plus Akron had elevated concentrations of Rb. Mandan also stood out with high Cr concentrations, while Akron exhibited high Zn and Tl concentrations in some samples. Dust from the remaining sites—CPER, El Reno, Jornada, and Moab—had low to moderate concentrations of all elements relative to other sites. Some notable trends in the dataset (including data from all sites) were strong positive correlations between Fe and Co ($R^2 = 0.94$), between Cs and Ba ($R^2 = 0.89$), and among the REEs. The REEs were correlated with each other across sites except for relatively high Eu concentrations at Red Hills and Mandan.

Given the large number of elements measured in our dataset and the wide geographic area of the study, it can be difficult to identify elements that create a distinct dust signature for each NWERN site. We used a cluster analysis, PCA, and LDA to evaluate geochemical variability across sites. The hierarchical cluster dendrogram (Fig. 2) separated dust from some of the sites based on Euclidean distance in the normalized geochemical data space. Samples from Twin Valley, Red Hills, Lordsburg, and Mandan plotted together within their respective sites in the dendrogram. Most of the Moab samples plotted together, with some overlapping samples from other sites. Likewise, most El Reno samples plotted together. The remaining sites were poorly grouped in the cluster analysis. Samples from CPER and Jornada were spread widest across the entire dendrogram. Samples from HAFB were spread across the right side of the dendrogram and samples from Akron were spread across the left side.

In the PCA, a plot of PC2 vs. PC1 (Fig. 3) visually separated dust from most of the sites but overlap existed between several sites. PC1 explained 56.9 % of the variation and was most dependent on Li, Co, Cd, Eu, La, Be, Ce, and Sm. PC2 explained 13.8 % of the variation and was most dependent on Fe, Mn, Li, Pr, Zn, Y, Se, and La. The HAFB samples clustered together on the negative end of PC1 and the Lordsburg samples clustered together on the positive end. Samples from Moab, Jornada, CPER, and El Reno also plotted toward the negative end of PC1 with a large spread and overlap among the sites. Samples from Red Hills, Twin Valley, Mandan, and Akron plotted toward the positive end of PC1 with similar spread and overlap across sites. PC2 effectively separated the playa-influenced sites, HAFB and Lordsburg, from the rest of the sites. The coefficients of PC1 and PC2 (linear combinations of the original variables that make up the PC) were not readily interpretable due to the plethora of variables, such that the element groups had no clear relationships. The overlap in elements contributing substantially to both PC1 and PC2 further complicated attributing specific dust source types to each PC. However, PC2 exhibited a proclivity to separate non-playa sites on the negative end and playa-influenced sites (HAFB and Lordsburg) on the positive end with relatively high concentrations of Li, Se, and REEs. Additional PCs described more variability in the dataset (6.0 % for PC3) but the plots of PC3 vs. PC1 or PC2 failed to offer additional insight into the sites beyond what was observed in Fig. 3.

The LDA using all geochemical data (Fig. 4) provided clear differentiation of dust from all sites in plots involving the first three linear discriminants because the method searches for directions that are useful for separation based on the site. The first three linear discriminants (LDs) described 80.7 % of variability in the geochemistry dataset, with

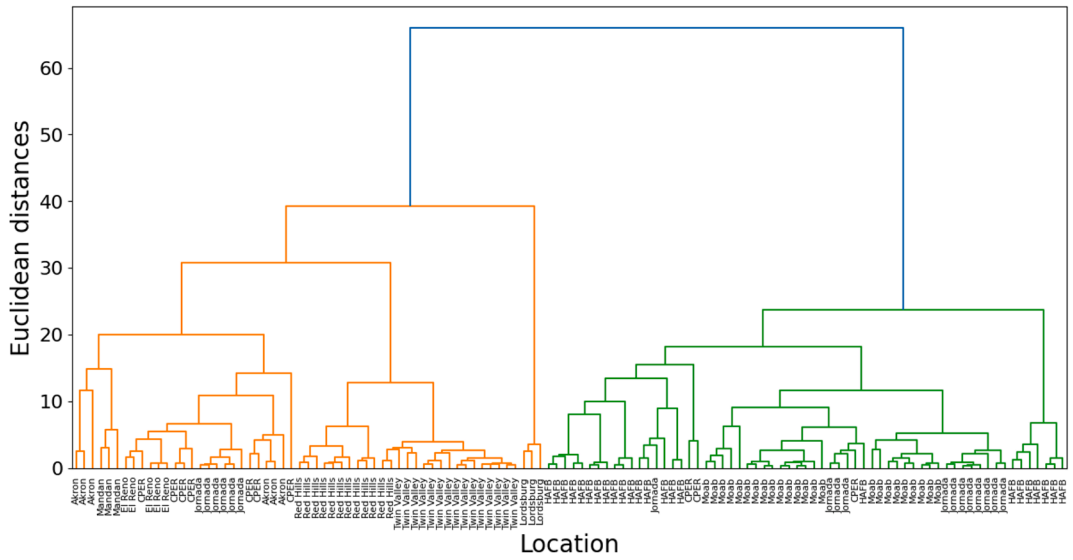

Fig. 2. Hierarchical clustering dendrogram for all composite dust samples from the ten National Wind Erosion Research Network (NWERN) sites using concentrations of 40+ trace and major elements.

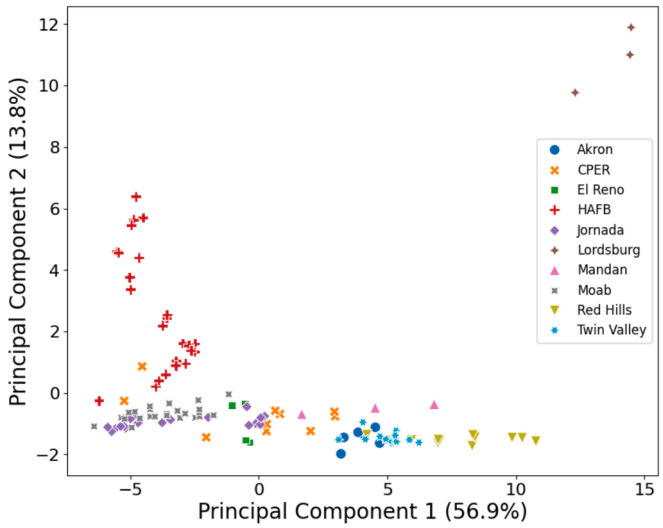

Fig. 3. Ordination plot of principal component 2 (PC2) vs. PC1 for principal component analysis (PCA) of all dust composite samples from the ten National Wind Erosion Research Network (NWERN) sites using concentrations of 40+ trace and major elements.

40.9 % from LD1, 22.1 % from LD2, and 17.7 % from LD3. LD1 was most dependent on Sm, U, Ce, Nd, Y, Rb, and Ho, LD2 was most dependent on La, Er, Rb, Ce, Y, Nd, and Ho, and LD3 was most dependent on Be, Ca, Yb, Gd, Rb, Sm, and Dy. LD1 mainly separated Lordsburg on the positive end from all other sites on the negative end (Fig. 4, top panel). LD2 distinguished most other sites (besides Lordsburg) with samples from individual sites clustering together and mostly not overlapping with samples from other sites (Fig. 4, top panel). However, there was considerable overlap between the samples from Jornada, Moab, and El Reno. For this reason, we included LD3 to differentiate these three sites. In the plot of LD3 vs. LD2 (Fig. 4, bottom panel), samples from El Reno, Jornada, and Moab were clearly distinguished from the negative to positive end along LD3. In fact, the plot of LD3 vs. LD2 (Fig. 4, bottom panel) differentiated nearly all the sites with only minor overlap between Red Hills and Twin Valley distributions, and the plot of LD2 vs. LD1 (Fig. 4, top panel) clearly differentiated dust from these sites.

The LDA clearly separated sites, but the elements (coefficients) describing LD1, LD2, and LD3 were not readily interpretable, likely because there were so many categories. Some of the same elements were influential for more than one LD, likely a consequence of the large number of variables involved and the algorithm using sites as target categories. Yet, the distribution of samples was similar to that of the PCA with Lordsburg plotting distinctly from the rest of the sites and similar arrangement of sites from HAFB to Twin Valley and Red Hills along PC1 (Fig. 3) and LD2 (Fig. 4, top panel). Though similar to PCA, the LDA was more successful at separating dust geochemistry from all the sites relative to the PCA. Further, the LDA model incorporating all geochemical data accurately predicted 100 % of the sample categories.

The LDA using REE + Y concentrations (Fig. 5) provided clear differentiation of dust from all sites in plots involving the first two linear discriminants. The first two LDs described 80.2 % of variability in the REE + Y dataset, with 66.1 % from LD1 and 14.1 % from LD2. LD1 mainly separated Lordsburg, Red Hills, and Twin Valley on the positive end from all other sites on the negative end, and further distinguished Akron, CPER, and Jornada. LD2 distinguished the other sites with samples from individual sites clustering together and mostly not overlapping with samples from other sites. Although the LDA model incorporating REE + Y data provided clear visual distinction of all sites in the plot of LD2 vs. LD1, the model misclassified one of the CPER samples as an HAFB sample. We conclude that the REE + Y elements are probably among the best for differentiating sites, but inclusion of other elements also has some value.

With three LDs in the LDA using all geochemical data, samples from each site were distinct from other sites regardless of the season in which samples were collected. However, some sites showed seasonal variability in the raw data. To further investigate potential seasonality of dust geochemistry, we performed a site-specific LDA for each site that had >10 samples (CPER, HAFB, Jornada, Moab, Red Hills, and Twin Valley) using the seasons as target categories. At each site, the spring, summer, and fall samples were clearly distinguished from each other with two LDs with HAFB shown as an example (Fig. 6). At HAFB, two LDs explained 100 % of variability in the site data with 70.6 % explained by LD1 and 29.4 % explained by LD2. The fall samples were differentiated from spring and summer samples along LD1, while the spring samples were differentiated along LD2. The coefficients indicating the largest elemental contributions to LD1 and LD2 were not easily interpreted, likely because there were so many categories. LD1 was most dependent on Na, Cs, Th, Be, and Co. LD2 was most dependent on Mg and As, which may reflect higher contributions from playa dust in the

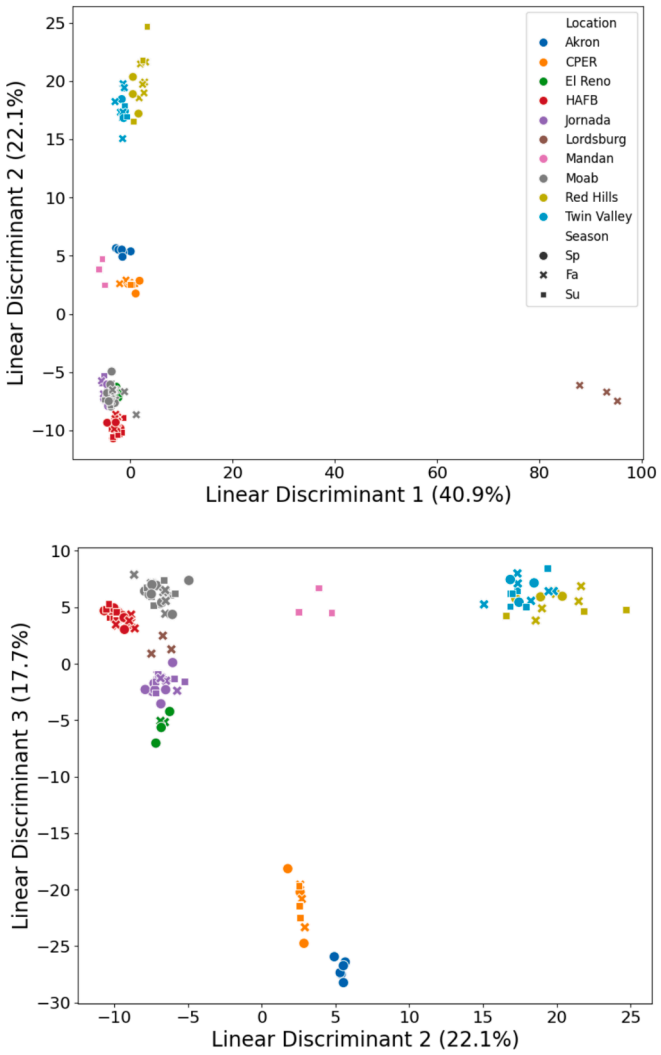

Fig. 4. Plots of linear discriminant 2 (LD2) vs. LD1 (top panel) and LD3 vs. LD2 (bottom panel) for linear discriminant analysis (LDA) of all composite dust samples from the ten National Wind Erosion Research Network (NWERN) sites using concentrations of 40+ trace and major elements. The symbols represent samples collected during spring, summer, and fall.

summer and fall samples relative to spring samples. Seasonally categorized LDAs for all six sites with >10 samples are presented in the Supplementary material.

3.3. Mineralogy shows common and distinct minerals among sites with seasonal variability

The mineralogy of NWERN dust was characterized by a common set of minerals at all or most sites with distinct mineral composition at some individual sites. All sites contained quartz, ranging from 22.7 ± 1 % (average ± std error) abundance at Twin Valley to 60 ± 2 % at Moab. Na-feldspars were the next most common mineral group, present at all sites except Moab and ranging in the remaining nine sites from 12 ± 3 % abundance at Twin Valley to 66 ± 4 % at Red Hills. Other feldspar minerals, calcic plagioclase (anorthite) and K-feldspars, were each found at five of the ten sites. The 2:1 phyllosilicates were also common, occurring at seven of the ten sites. The next most common minerals were muscovite and calcite, each found at five of ten sites. HAFB dust had distinctive mineralogy because the site is located downwind of playas and dunes of White Sands National Park and was the only dust that contained calcium sulfate minerals (anhydrite and bassanite), chloride

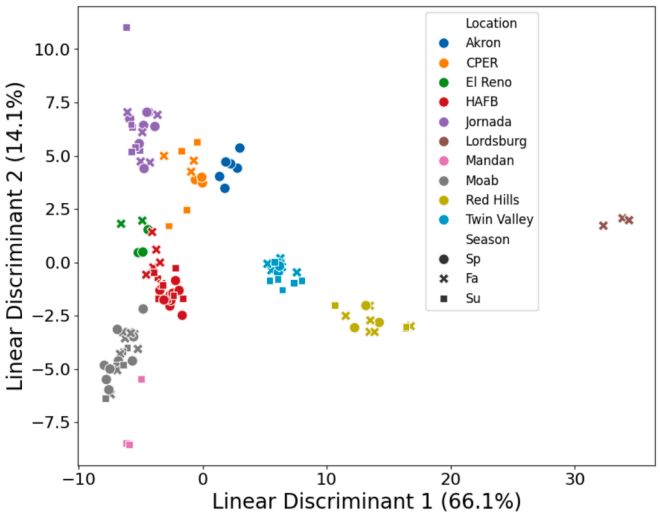

Fig. 5. Plot of linear discriminant 2 (LD2) vs. LD1 for linear discriminant analysis (LDA) of all composite dust samples from the ten National Wind Erosion Research Network (NWERN) sites using rare earth element (REE) + Y concentrations. The symbols represent samples collected during spring, summer, and fall.

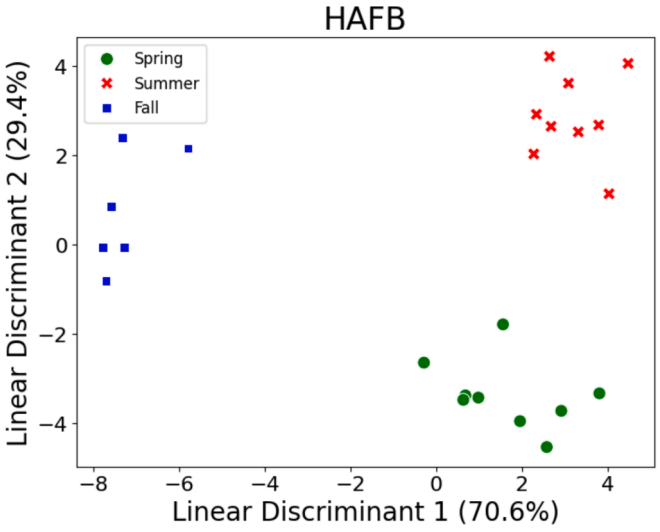

Fig. 6. Plot of linear discriminant 2 (LD2) vs. LD1 for the site-specific linear discriminant analysis (LDA) to highlight seasonal differences in geochemistry at Holloman Air Force Base (HAFB) using concentrations of 40+ trace and major elements. Seasonal-categorized LDAs for all sites with >10 composite dust samples are provided in the Supplementary material.

salts (halite and sylvite), and iron oxides (magnetite and hematite). Mandan was the only site that contained aluminite. Moab and Jornada were the only sites with smectite clays.

Two sites, El Reno and HAFB, demonstrated seasonal variability in their mineral composition. El Reno dust contained gypsum, calcite, and dolomite in spring but not fall. In contrast, the fall dust samples at El Reno contained calcic plagioclase (anorthite) that was absent in the spring. HAFB dust had a similar mineral composition in the spring and summer samples but with different relative abundances of nearly all minerals. The summer dust at HAFB contained more quartz and Na-feldspar, while the spring samples contained more anhydrite and bassanite. Other sites potentially had seasonal differences in mineral assemblages, but we did not have seasonal samples at all sites (sample periods shown in Supplementary material, Table S1).

LDA offered the ability to visualize differences in mineralogy using

sites as target categories (Fig. 7). The first three LDs explained 86.3 % of the variability in the mineralogy dataset and separated most sites from one another. LD1 (50.6 % of the variability) distinguished HAFB and Lordsburg from everything else. LD2 (26.0 %) primarily separated Lordsburg from the other sites. LD3 (9.7 %) separated most of the other sites, but not in all cases, and the discriminant model misclassified a small percentage of dust samples.

It is remarkable how well the sites plotted distinctly from each other in LD space (Fig. 7) given the relatively small number of variables (mineral phases) in the dataset. LD1 was most dependent on sylvite, gypsum, and magnetite on the positive end, with sodic plagioclase, calcic plagioclase, and quartz on the negative end. LD2 was most dependent on 2:1 phyllosilicates, gypsum, and magnetite on the positive end, with bassanite (calcium sulfate), sodic plagioclase, calcite, and quartz on the negative end. LD3 was most dependent on aluminite, dolomite, gypsum, magnetite, and kaolinite on the positive end. These groups of minerals are related to the local bedrock geology or surficial sediments at the sample sites.

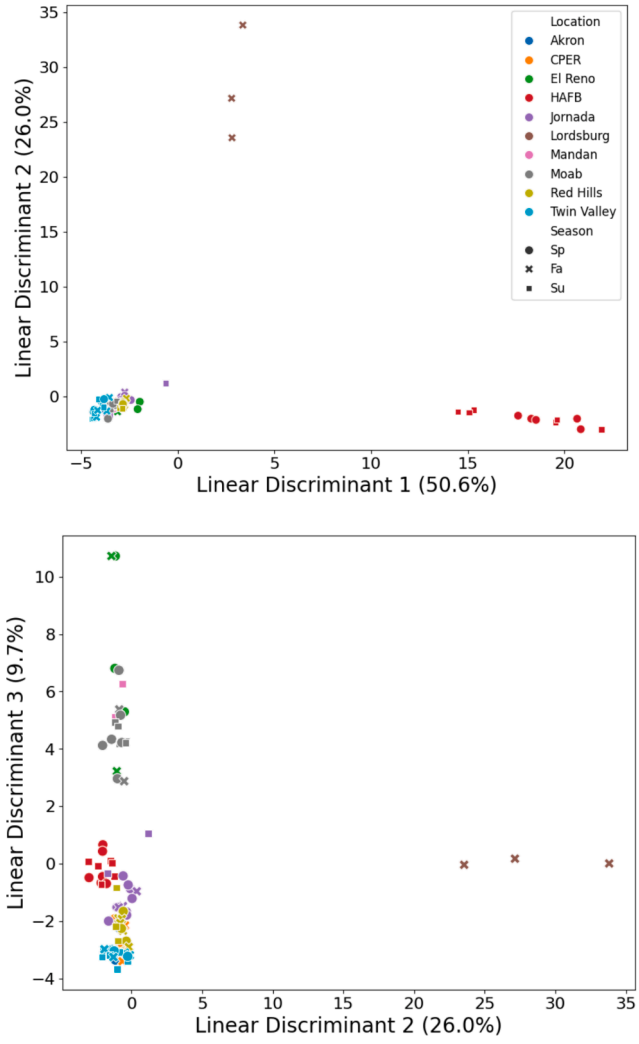

Fig. 7. Plots of linear discriminant 2 (LD2) vs. LD1 (top panel) and LD3 vs. LD2 (bottom panel) for linear discriminant analysis (LDA) of all composite samples from the ten National Wind Erosion Research Network (NWERN) sites using mineral abundances. The symbols represent samples collected during spring, summer, and fall.

4. Discussion

4.1. Geochemical and mineralogical signatures of representative dust sources

The geochemical and mineralogical data were useful for separating dust emissions among NWERN sites. We found that the LDA based on geochemistry (Fig. 4) was the best way to visually differentiate dust across the sites because it provided the clearest distinction among sites compared with PCA, cluster analysis, and the LDA based on mineralogy. The LDA model based on REE + Y concentrations (Fig. 5) likewise provided clear visual distinction between all sites in LDA plots, although it was slightly less accurate because it misclassified one sample. The LDA model based on geochemistry provided clear distinction of all sites with three LDs while the LDA model based on REE + Y concentrations provided clear distinction of all sites with only two LDs. For source apportionment, a dust deposition sample plotted on the LDA diagrams may be closely tied to one of the sites or a mixture of the sites. We suggest that LDA represents an underutilized statistical tool for dust tracing studies, and the LDA could be based on a full suite of geochemical data or a subset of REE + Y data. However, the elements describing each LD were not readily interpretable, with some elements contributing substantially to more than one LD. The LDA using mineralogical data provided somewhat less distinction among sites, but the coefficients were more easily interpretable given the smaller number of variables.

The underlying lithology is the primary control on dust geochemistry and mineralogy at the NWERN sites. In the PCA and LDA plots, dust samples were clustered based on the age and type of bedrock or sediments underlying the sample sites. For example, in the PCA, PC1 indicated a gradient of sites with more weathered sand, sandstone, or alluvium (Moab and Jornada) on the negative end to sites with less-weathered, younger volcanic bedrock or lacustrine sediments on the positive end (Twin Valley, Red Hills, and Lordsburg), reflected by relatively high concentrations of Li, Co, Cd, Be, and REEs. PC2 exhibited a proclivity to separate non-playa sites on the negative end and playa-influenced sites (HAFB and Lordsburg) on the positive end with relatively high concentrations of Li, Se, and REEs. In the LDAs with all geochemical data and REE + Y concentrations, the sites plotted similarly to the PCA differentiated according to the degree of weathering. For example, dust from sites with younger volcanic bedrock (e.g., Twin Valley and Red Hills) plotted separately from sites with more weathered bedrock or sediments (e.g., HAFB, Jornada, and Moab). The sites also plotted similarly in the LDA based on mineralogy, with the advantage that the discriminant coefficients were more readily interpretable in terms of the geologic settings of the sites compared with the PCA and LDAs based on geochemical data. Sites located near playas or gypsum sand dunes (HAFB and Lordsburg, with higher abundances of weathering products sylvite and gypsum) were separated from the rest of the sites (with higher abundances of primary minerals plagioclase and quartz) along LD1, while sites with young volcanic bedrock (Red Hills and Twin Valley) were separated from sites with older, more weathered bedrock (Moab, El Reno, and Mandan) along LD2.

The relationship between dust composition and underlying lithology has been demonstrated in other studies. For example, a study of 28 potential dust source areas across the western US found that differences in trace metal concentrations and radiogenic isotopes (Sr, Nd, Hf) were related to geologic provinces (Aarons et al., 2017). The major element composition of Gobi Desert dust sources was linked to source rocks and mineral maturity related to the supply of fresh materials (Zhao et al., 2019). The composition of dust emissions from playas across western Utah was dominated by evaporite minerals and associated elements (Li, Na, Sr, U, Mg, and Ca) (Goodman et al., 2019). In addition to the local lithology of dust sources, dust geochemistry may be impacted by anthropogenic sources like mining or human-influenced playas (Reheis et al., 2002). In our study of NWERN dust, the local bedrock is the main

factor determining separation of sites in the PCA and LDA analyses, but there is evidence for anthropogenic pollution. Elevated Cu in Lordsburg dust, Ni and Mo in HAFB dust, Zn and Tl in Akron dust, and Cr in Mandan dust suggest anthropogenic influences on dust composition at these sites. However, it is not clear whether the metal pollution was from local sources or deposited on nearby soils and advected to our samplers.

One drawback of using geochemical or mineralogical tracers of dust was the inability to distinguish between cropland and rangeland sites because these tracers are controlled predominantly by the underlying geology, irrespective of land use. The playa-influenced dust at Lordsburg and HAFB, however, was clearly distinguished from dust at the cropland and rangeland sites because of the abundance of evaporite minerals and associated elements. The lack of differences between the dust geochemistry and mineralogy from cropland and rangeland sites suggests that additional tracers are needed to differentiate sites based on land use. For example, nutrient chemistry (Brahney et al., 2014; Heindel et al., 2020), isotopic measurements that distinguish sources from fertilizers or other chemicals used in farming (Qu and Han, 2023), or bacteria and fungi (Barberán et al., 2015; Grantham et al., 2015) may be used to further separate sites. We explored the utility of using core microbiome communities as a novel dust signature on the same set of samples in a companion study (Leifi, 2022).

As an example of how dust signatures may be developed from multiple data sources, we compared the proximal Nevada sites (Red Hills and Twin Valley), the proximal Colorado sites (Akron and CPER), and the proximal New Mexico sites (Jornada and HAFB). Red Hills and Twin Valley dust samples overlapped on the PCA plot and the LDA plot with mineralogy, plotted nearby on the clustering dendrogram, but plotted distinctly on the LDA plots based on all geochemical data (Fig. 4) and REE + Y concentrations (Fig. 5). Dust samples from Akron and CPER overlapped in the clustering dendrogram and LDA plot with mineralogy but were distinct in the PCA plot (Fig. 3) and LDA plots with geochemistry (Figs. 4 and 5). Jornada and HAFB were mixed on the clustering dendrogram but were clearly distinguished in the PCA plot (Fig. 3), LDA plots with geochemistry (Figs. 4 and 5), and LDA plot with mineralogy (Fig. 7). The mineral abundances provided the clearest distinction for Jornada and HAFB. In all cases, the combination of geochemistry and mineralogy was sufficient to separate the sites given variability in underlying lithology. In cases where the lithology or surficial sediments are similar across potential dust source areas, additional tracers may be necessary to differentiate sites. For example, playa dust sources in western Utah contained similar mineral assemblages and geochemistry (Goodman et al., 2019) and could only be differentiated by $^{87}Sr/^{86}Sr$ ratios in carbonate minerals (Carling et al., 2020).

Our results demonstrate that geochemical and mineralogical measurements at potential dust source areas could plausibly be used to separate dust composition between proximal sites and across large geographical areas with variable underlying geology. The sites investigated here are representative of common types of dust sources, but to use source composition to unmix a dust sample, dust composition libraries would need to include all relevant regional dust sources and a distribution of geochemical variability within sources areas. The potential sources contributing to dust deposition at any site would likely include dust-emitting landscapes that are not contained in our dataset or other compilations. To use these types of compilations for unmixing dust samples, regional dust sources should be first investigated as the dust supply at most localities reflects nearby sites more than far-flung sites. For example, dust deposition to the San Juan Mountains in Colorado contained regional dust, with only a small fraction of Asian dust, based on particle size distributions and back-trajectories (Lawrence et al., 2010). Similarly, dust deposition to mountains in Idaho, Nevada, and Utah was dominated by regional rather than global dust sources, based on geochemical measurements combined with particle size distributions and back-trajectories (Munroe et al., 2023).

4.2. Seasonality of geochemical signatures

Seasonal variability of dust geochemistry and mineralogy was evident within sites, demonstrating challenges with developing signatures of dust sources. In the LDA plots based on geochemistry and with dust samples categorized by season (Fig. 6 for HAFB and Supplementary material for the other sites), the spring, summer, and fall samples were clearly distinguished from one another. Dust sources may change seasonally with changing wind directions, disturbance (e.g., fire), changes in land use (e.g., grazing or mining), vegetation cover, or water cover (Chappell et al., 2023; Gill, 1996; Miller et al., 2012). Dust at the HAFB site exhibited seasonal differences in mineralogy between spring and fall with SW prevailing winds in the spring and SSE prevailing winds in the fall. The spring samples were likely more influenced by gypsum from White Sands National Park, whereas the fall samples likely received more dust from sources to the west of the site. Also, the Twin Valley and Red Hills sites were burned by wildfire prior to dust collection in our study, which may have impacted how dust was emitted from the sites and what types of minerals were contained in our samples.

Although seasonal variability was evident at some sites, the signatures developed using geochemistry and mineralogy data were robust because the seasonal variability was clearly much less important than across-site variability. In the LDA plots with geochemistry (Figs. 4 and 5) and LDA plot with mineralogy (Fig. 7), the sites cluster together regardless of season, suggesting seasonal variability was apparent but not essential to identifying a dust signature.

4.3. Implications for dust tracing studies

Our study highlights the complexity of developing geochemical signatures of dust sources over large regions with various controls on dust geochemistry and mineralogy. Even with these complexities, the dataset presented here (Mangum et al., 2024) is a step toward building a library of dust composition for key dust sources across the western US that may improve dust tracing from source to sink, building on previous studies at potential source areas (Aarons et al., 2017; Carling et al., 2020; Goodman et al., 2019). These types of libraries can be used to trace dust back to its source, such as linking alpine dust deposition in the Uinta Mountains to source areas in the southwestern US (Munroe et al., 2019). Whereas many studies rely on isotopic measurements, we demonstrate that dust from diverse NWERN sites may be differentiated based on geochemistry and mineralogy. Specific combinations of variables may be used in tandem to highlight differences and act as a dust signature across seasons.

The main implications of our study are:

1) Geochemistry and mineralogy successfully separated representative dust sources across the western US. Geochemistry worked better than mineralogy for separating sites, but the mineralogy differences were more easily interpreted with respect to the underlying geology.
2) Linear discriminant plots successfully distinguished all sites using all geochemical data and a subset of REE + Y concentrations. The LDA using mineralogical data distinguished most sites with a smaller number of variables as inputs. We suggest that LDA is a useful, but underutilized, tool for separating geochemistry and mineralogy across dust sources.
3) The LDA using only REE + Y data separated all sites in plots using only two LDs, compared with three LDs in the LDA using all geochemical data, but was slightly less accurate at classifying sites.
4) Principal component analysis (PCA) and cluster analysis, two commonly used statistical methods for visualizing geochemical data, did not provide sufficient discrimination for samples among all sites.
5) Across-site variability in geochemistry and mineralogy was more important than seasonal variability.
6) Playa dust was easily recognizable based on its distinct mineralogy and geochemistry. We were unable to differentiate dust from

cropland and rangeland sites using mineralogy and geochemistry, highlighting the need for additional tracers to distinguish dust sources based on land use.

Our dataset and statistical analyses presented here describe methods for successfully characterizing representative dust sources across the western US. Dust tracing studies require a library of geochemical and mineralogical data to differentiate dust sources. Geochemistry and mineralogy sufficiently separated dust sources based on differences in lithology, and other tracers could be used to further differentiate sites based on land use. Additional data are needed to build libraries of potential dust sources across arid regions of the world. With new information on the sources contributing to dust fluxes to urban and alpine areas, dust sources may be identified and remediated to prevent the adverse effects of windblown dust.

CRediT authorship contribution statement

Abby L. Mangum: Writing – original draft, Methodology, Formal analysis, Data curation. **Gregory T. Carling:** Writing – review & editing, Writing – original draft, Validation, Supervision, Resources, Project administration, Methodology, Investigation, Funding acquisition, Formal analysis, Data curation, Conceptualization. **Barry R. Bickmore:** Writing – review & editing, Writing – original draft, Validation, Supervision, Methodology, Investigation, Funding acquisition, Formal analysis, Conceptualization. **Nicholas Webb:** Writing – review & editing, Resources, Methodology, Investigation, Data curation, Conceptualization. **DeTiare L. Leifi:** Methodology, Investigation. **Janice Brahney:** Writing – review & editing, Supervision, Investigation, Conceptualization. **Diego P. Fernandez:** Supervision, Methodology, Data curation. **Kevin A. Rey:** Supervision, Methodology, Investigation, Data curation. **Stephen T. Nelson:** Supervision, Methodology, Investigation. **Landon Burgener:** Writing – review & editing, Supervision. **Joshua J. LeMonte:** Writing – review & editing, Supervision, Methodology. **Alyssa N. Thompson:** Methodology, Investigation. **Beth A. Newingham:** Writing – review & editing, Resources, Methodology, Investigation. **Michael C. Duniway:** Writing – review & editing, Methodology, Conceptualization. **Zachary T. Aanderud:** Writing – review & editing, Supervision, Resources, Project administration, Methodology, Investigation, Funding acquisition, Conceptualization.

Declaration of competing interest

The authors declare that they have no known competing financial interests or personal relationships that could have appeared to influence the work reported in this paper.

Data availability

All data are published in the EarthChem data repository. The data citation is provided in the article.

Acknowledgments

This work was supported by the US National Science Foundation grants EAR-2012093 and EAR-2005432. All data used in the study are available in the EarthChem repository (https://doi.org/10.26022/IEDA/112945). Samples were provided by investigators at the National Wind Erosion Research Network sites. We especially thank Justin Van Zee, Ericha Courtright, and Brad Cooper for NWERN sample and data curation. The National Wind Erosion Research Network is part of the Long-Term Agroecosystem Research (LTAR) network supported by the US Department of Agriculture (USDA). Any use of trade, firm, or product names is for descriptive purposes only and does not imply endorsement by the US Government.

Appendix A. Supplementary data

Supplementary data to this article can be found online at https://doi.org/10.1016/j.aeolia.2024.100941.

References

Aarons, S.M., Blakowski, M.A., Aciego, S.M., Stevenson, E.I., Sims, K.W.W., Scott, S.R., Aarons, C., 2017. Geochemical characterization of critical dust source regions in the American West. Geochim. Cosmochim. Acta 215, 141–161.
Abed, R.M.M., Ramette, A., Hübner, V., De Deckker, P., de Beer, D., 2012. Microbial diversity of eolian dust sources from saline lake sediments and biological soil crusts in arid Southern Australia. FEMS Microbiol. Ecol. 80, 294–304.
Barberán, A., Ladau, J., Leff, J.W., Pollard, K.S., Menninger, H.L., Dunn, R.R., Fierer, N., 2015. Continental-scale distributions of dust-associated bacteria and fungi. Proc. Natl. Acad. Sci. 112, 5756–5761.
Belnap, J., Reynolds, R.L., Reheis, M.C., Phillips, S.L., Urban, F.E., Goldstein, H.L., 2009. Sediment losses and gains across a gradient of livestock grazing and plant invasion in a cool, semi-arid grassland, Colorado Plateau, USA. Aeolian Res. 1, 27–43.
Belnap, J., Walker, B.J., Munson, S.M., Gill, R.A., 2014. Controls on sediment production in two U.S. deserts. Aeolian Res. 14, 15–24.
Ben-Israel, M., Enzel, Y., Amit, R., Erel, Y., 2015. Provenance of the various grain-size fractions in the Negev loess and potential changes in major dust sources to the Eastern Mediterranean. Quat. Res. 88, 105–115.
Blakowski, M.A., Aciego, S.M., Delmonte, B., Baroni, C., Salvatore, M.C., Sims, K.W.W., 2016. A Sr-Nd-Hf isotope characterization of dust source areas in Victoria Land and the McMurdo Sound sector of Antarctica. Quat. Sci. Rev. 141, 26–37.
Brahney, J., Ballantyne, A.P., Kociolek, P., Spaulding, S., Otu, M., Porwoll, T., Neff, J.C., 2014. Dust mediated transfer of phosphorus to alpine lake ecosystems of the Wind River Range, Wyoming, USA. Biogeochemistry 120, 259–278.
Brahney, J., Ballantyne, A.P., Kociolek, P., Leavitt, P.R., Farmer, G.L., Neff, J.C., 2015. Ecological changes in two contrasting lakes associated with human activity and dust transport in western Wyoming. Limnol. Oceanogr. 60, 678–695.
Brahney, J., Ballantyne, A.P., Vandergoes, M., Baisden, T., Neff, J.C., 2019. Increased dust deposition in new zealand related to twentieth century Australian land use. J. Geophys. Res. Biogeo. 124, 1181–1193.
Carling, G.T., Fernandez, D.P., Rey, K.A., Hale, C.A., Goodman, M.M., Nelson, S.T., 2020. Using strontium isotopes to trace dust from a drying Great Salt Lake to adjacent urban areas and mountain snowpack. Environ. Res. Lett. 15, 114035.
Chappell, A., Webb, N.P., Hennen, M., Schepanski, K., Ciais, P., Balkanski, Y., Zender, C. S., Tegen, I., Zeng, Z., Tong, D., Baker, B., Ekström, M., Baddock, M., Eckardt, F.D., Kandakji, T., Lee, J.A., Nobakht, M., von Holdt, J., Leys, J.F., 2023. Satellites reveal Earth's seasonally shifting dust emission sources. Sci. Total Environ. 883, 163452.
Chen, J., Li, G., 2011. Geochemical studies on the source region of Asian dust. Sci. China Earth Sci. 54, 1279–1301.
Chen, H., Wu, D., Wang, Q., Fang, L., Wang, Y., Zhan, C., Zhang, J., Zhang, S., Cao, J., Qi, S., Liu, S., 2022. The predominant sources of heavy metals in different types of fugitive dust determined by principal component analysis (PCA) and positive matrix factorization (PMF) modeling in southeast hubei: a typical mining and metallurgy area in Central China. Int. J. Environ. Res. Public Health 19, 13227.
Dastrup, D.B., Carling, G.T., Collins, S.A., Nelson, S.T., Fernandez, D.P., Tingey, D.G., Hahnenberger, M., Aanderud, Z.T., 2018. Aeolian dust chemistry and bacterial communities in snow are unique to airshed locations across northern Utah, USA. Atmos. Environ. 193, 251–261.
Davis, J.C., 2002. Statistics and Data Analysis in Geology. Wiley, New York.
Doelling, H.H., 2002. Geologic Map of the Moab and Eastern part of the San Rafael desert 30'X 60' quadrangles, Grand and Emery counties, Utah, and Mesa county, Colorado. Utah Geological Survey, Salt Lake City, Utah.
Duniway, M.C., Pfennigwerth, A.A., Fick, S.E., Nauman, T.W., Belnap, J., Barger, N.N., 2019. Wind erosion and dust from US drylands: a review of causes, consequences, and solutions in a changing world. Ecosphere 10, e02650.
Eberl, D.D., 2003. User's guide to RockJock – A program for determining quantitative mineralogy from powder X-ray diffraction data, U.S. Geological Survey Open-File Report 2003-78.
Esri, 2024. ArcGIS Pro (Version 3.0). In: Inc., E. (Ed.).
Gill, T.E., 1996. Eolian sediments generated by anthropogenic disturbance of playas: human impacts on the geomorphic system and geomorphic impacts on the human system. Geomorphology 17, 207–228.
Goodman, M.M., Carling, G.T., Fernandez, D.P., Rey, K.A., Hale, C.A., Bickmore, B.R., Nelson, S.T., Munroe, J.S., 2019. Trace element chemistry of atmospheric deposition along the Wasatch Front (Utah, USA) reflects regional playa dust and local urban aerosols. Chem. Geol. 530, 119317.
Goossens, D., Offer, Z.Y., 2000. Wind tunnel and field calibration of six aeolian dust samplers. Atmos. Environ. 34, 1043–1057.
Grantham, N.S., Reich, B.J., Pacifici, K., Laber, E.B., Menninger, H.L., Henley, J.B., Barberán, A., Leff, J.W., Fierer, N., Dunn, R.R., 2015. Fungi identify the geographic origin of dust samples. PLoS One 10, e0122605.
Grousset, F.E., Biscaye, P.E., 2005. Tracing dust sources and transport patterns using Sr, Nd and Pb isotopes. Chem. Geol. 222, 149–167.
Guinoiseau, D., Singh, S.P., Galer, S.J.G., Abouchami, W., Bhattacharyya, R., Kandler, K., Bristow, C., Andreae, M.O., 2022. Characterization of Saharan and Sahelian dust sources based on geochemical and radiogenic isotope signatures. Quat. Sci. Rev. 293, 107729.

Heindel, R.C., Putman, A.L., Murphy, S.F., Repert, D.A., Hinckley, E.L.S., 2020. Atmospheric dust deposition varies by season and elevation in the Colorado front range, USA. J. Geophys. Res. Earth 125, e2019JF005436.
Hubbard, C.R., Evans, E.H., Smith, D.K., 1976. The reference intensity ratio, I/Ic, for computer simulated powder patterns. J. Appl. Cryst. 9, 169–174.
Kellogg, C.A., Griffin, D.W., 2006. Aerobiology and the global transport of desert dust. Trends Ecol. E 21, 638–644.
Lawrence, C.R., Neff, J.C., 2009. The contemporary physical and chemical flux of aeolian dust: a synthesis of direct measurements of dust deposition. Chem. Geol. 267, 46–63.
Lawrence, C.R., Painter, T.H., Landry, C.C., Neff, J.C., 2010. Contemporary geochemical composition and flux of aeolian dust to the San Juan Mountains, Colorado, United States. J. Geophys. Res. 115, G03007.
Leifi, D.L., 2022. Core Microbiome to Fingerprint Dust Emission Sources Across the Western USA. Brigham Young University, Provo, UT.
Mangum, A.L., Carling, G., Nelson, S., Fernandez, D., 2024. Characterizing Dust from National Wind Erosion Research Network Sites Using Strontium Isotopes, Major and Trace Element Chemistry, and Mineralogy, Version 1.0., Interdisciplinary Earth Data Alliance (IEDA).
Marcy, M.J., Carling, G.T., Thompson, A.N., Bickmore, B.R., Nelson, S.T., Rey, K.A., Fernandez, D.P., Heiner, M., Adams, B.R., 2024. Trace element chemistry and strontium isotope ratios of atmospheric particulate matter reveal air quality impacts from mineral dust, urban pollution, and fireworks in the Wasatch Front, Utah, USA. Appl. Geochem. 162, 105906.
Marx, S.K., Kamber, B.S., McGowan, H.A., 2008. Scavenging of atmospheric trace metal pollutants by mineral dusts: inter-regional transport of Australian trace metal pollution to New Zealand. Atmos. Environ. 42, 2460–2478.
McTainsh, G., Strong, C., 2007. The role of aeolian dust in ecosystems. Geomorphology 89, 39–54.
Menéndez, I., Pérez-Chacón, E., Mangas, J., Tauler, E., Engelbrecht, J.P., Derbyshire, E., Cana, L., Alonso, I., 2014. Dust deposits on La Graciosa Island (Canary Islands, Spain): texture, mineralogy and a case study of recent dust plume transport. Catena 117, 133–144.
Middleton, N.J., Goudie, A.S., 2001. Saharan dust: sources and trajectories. Trans. Inst. Br. Geogr. 26, 165–181.
Miller, M.E., Bowker, M.A., Reynolds, R.L., Goldstein, H.L., 2012. Post-fire land treatments and wind erosion – lessons from the Milford Flat Fire, UT, USA. Aeolian Res. 7, 29–44.
Miser, H.D., 1954. Geologic Map of Oklahoma. U.S. Department of the Interior, Reston, VA.
Munroe, J.S., Norris, E.D., Carling, G.T., Beard, B.L., Satkoski, A.M., Liu, L., 2019. Isotope fingerprinting reveals western North American sources of modern dust in the Uinta Mountains, Utah, USA. Aeolian Res. 38, 39–47.
Munroe, J.S., Soderstrom, E.J., Kluetmeier, C.L., Tappa, M.J., Mallia, D.V., Bauer, A.M., 2023. Regional sources control dust in the mountain critical zone of the Great Basin and Rocky Mountains, USA. Environ. Res. Lett. 18, 104034.
Murphy, E.C., 1999. Surface geology of mandan quadrangle, North Dakota. North Dakota Geological Survey, Bismarck, ND.
Nakano, T., Yokoo, Y., Nishikawa, M., Koyanagi, H., 2004. Regional Sr–Nd isotopic ratios of soil minerals in northern China as Asian dust fingerprints. Atmos. Environ. 38, 3061–3067.
Neff, J.C., Ballantyne, A.P., Farmer, G.L., Mahowald, N.M., Conroy, J.L., Landry, C.C., Overpeck, J.T., Painter, T.H., Lawrence, C.R., Reynolds, R.L., 2008. Increasing eolian dust deposition in the western United States linked to human activity. Nat. Geosci. 1, 189–195.
Ogden, T., 1979. Geologic Map of Colorado. U.S. Department of the Interior, Reston, Va.
Painter, T.H., Deems, J.S., Belnap, J., Hamlet, A.F., Landry, C.C., Udall, B., 2010. Response of Colorado River runoff to dust radiative forcing in snow. PNAS 107, 17125–17130.
Pedregosa, F., Varoquaux, G., Gramfort, A., Vincent Michel, B.T., Grisel, Olivier, Blondel, Mathieu, Prettenhofer, Peter, Weiss, Ron, Dubourg, Vincent, Vanderplas, Jake, Passos, Alexandre, Cournapeau, David, Brucher, Matthieu, Perrot, Matthieu, Duchesnay, Édouard, 2011. Scikit-learn: machine learning in python. J. Mach. Learn. Res. 12, 2825–2830.
Pierre, C., Bergametti, G., Marticorena, B., Mougin, E., Bouet, C., Schmechtig, C., 2012. Impact of vegetation and soil moisture seasonal dynamics on dust emissions over the Sahel. J. Geophys. Res. Atmospheres 117.
Prospero, J.M., Ginoux, P., Torres, O., Nicholson, S.E., Gill, T.E., 2002. Environmental characterization of global sources of atmospheric soil dust identified with the nimbus 7 total ozone mapping spectrometer (TOMS) absorbing aerosol product. Rev. Geophys. 40, 2-1–2-31.
Putman, A.L., Jones, D.K., Blakowski, M.A., DiViesti, D., Hynek, S.A., Fernandez, D.P., Mendoza, D., 2022. Industrial Particulate Pollution and Historical Land Use Contribute Metals of Concern to Dust Deposited in Neighborhoods Along the Wasatch Front, UT, USA. GeoHealth 6, e2022GH000671.
Qu, R., Han, G., 2023. Potassium isotopes of fertilizers as potential markers of anthropogenic input in ecosystems. Environ. Chem. Lett. 21, 41–45.
Reheis, M.C., Budahn, J.R., Lamothe, P.J., 2002. Geochemical evidence for diversity of dust sources in the southwestern United States. Geochim. Cosmochim. Acta 66, 1569–1587.
Reheis, M.C., Budahn, J.R., Lamothe, P.J., Reynolds, R.L., 2009. Compositions of modern dust and surface sediments in the Desert Southwest, United States. J. Geophys. Res.-Earth Surf. 114, 20.
Scholle, P.A., 2003. Geologic Map of New Mexico. New Mexico Bureau of Geology and Mineral Resources, Socorro, NM.
Skiles, S.M., Painter, T.H., Belnap, J., Holland, L., Reynolds, R.L., Goldstein, H.L., Lin, J., 2015. Regional variability in dust-on-snow processes and impacts in the Upper Colorado River Basin. Hydrol. Process. 29, 5397–5413.
Stewart, J.H., Carlson, J.E., 1978. Geologic Map of Nevada. U.S. Geological Survey and Nevada Bureau of Mines and Geology.
USGS, 2005. Selection of colors and patterns for geologic maps of the U.S. Geological Survey.
Webb, N.P., Herrick, J.E., Van Zee, J.W., Hugenholtz, C.H., Zobeck, T.M., Okin, G.S., 2015. Standard methods for wind erosion research and model development: protocol for the National Wind Erosion Research Network.
Webb, N.P., Herrick, J.E., Van Zee, J.W., Courtright, E.M., Hugenholtz, C.H., Zobeck, T. M., Okin, G.S., Barchyn, T.E., Billings, B.J., Boyd, R., Clingan, S.D., Cooper, B.F., Duniway, M.C., Derner, J.D., Fox, F.A., Havstad, K.M., Heilman, P., LaPlante, V., Ludwig, N.A., Metz, L.J., Nearning, M.A., Norfleet, M.L., Pierrson, F.B., Sanderson, M.A., Sharratt, B.S., Steiner, J.L., Tatarko, J., Tedela, N.H., Toledo, D., Unnasch, R.S., Van Pelt, S., Wagner, L., 2016. The National Wind Erosion Research Network: building a standardized long-term data resource for aeolian research, modeling and land management. Aeolian Res. 22, 23–36.
Webb, N.P., Chappell, A., Edwards, B.L., McCord, S.E., Van Zee, J.W., Cooper, B.F., Courtright, E.M., Duniway, M.C., Sharratt, B., Tedela, N., Toledo, D., 2019. Reducing sampling uncertainty in aeolian research to improve change detection. J. Geophys. Res. Earth 124, 1366–1377.
Zeng, W., Wan, X., Wang, L., Lei, M., Chen, T., Gu, G., 2022. Apportionment and location of heavy metal(loid)s pollution sources for soil and dust using the combination of principal component analysis, Geodetector, and multiple linear regression of distance. J. Hazard. Mater. 438, 129468.
Zenodo, 2024. The pandas development team.
Zhang, J., 1994. Atmospheric wet deposition of nutrient elements: correlation with harmful biological blooms in Northwest Pacific Coastal Zones. Ambio 23, 464–468.
Zhao, W., Sun, Y., Balsam, W., Zeng, L., Lu, H., Otgonbayar, K., Ji, J., 2015. Clay-sized Hf-Nd-Sr isotopic composition of Mongolian dust as a fingerprint for regional to hemispherical transport. Geophys. Res. Lett. 42, 5661–5669.
Zhao, W., Liu, L., Chen, J., Ji, J., 2019. Geochemical characterization of major elements in desert sediments and implications for the Chinese loess source. Sci. China Earth Sci. 62, 1428–1440.